assignment of the signal in compounds as complex as cobalamins.[5] The relationship between the assigned shifts and structure could be helpful in studies of B_{12} holoenzymes.

Several approaches have been employed to interpret ^{13}C shifts either as a function of structure[3] or as a function of the electronic influence of the R axial substituent.[7,19] These effects are closely, although probably not directly, related since good electron donor R groups lead to upfield ^{13}C NMR shifts of axial L that closely parallel increases in Co-L bond lengths.

Since H^+ is a pure electrophile, Brown suggested[8] that the effects of the H^+ give some indication of the consequences of electron withdrawal, particularly for C atoms remote from BN3. We compare (Table VI) the effect of $Co(CHEL)CH_3$ and H^+ on the ^{13}C shifts of Me_3Bzm. It is noteworthy that B9 is most affected by H^+, shifting upfield by ca. 13 ppm. All the $Co(CHEL)CH_3$ moieties shift this signal upfield; the Costa complexes have roughly similar effects, which are slightly greater than that of the $Co(DH)_2CH_3$ moiety. The same relationship holds for B5, B6, B7, and B12 shifts, which are futher downfield for Costa-type compounds than cobaloximes, consistent with the lower electrophilicity of Co in the latter. However, the B8 shift (which should be minimally affected by anisotropy) is anomalous in the Costa-type system, shifting downfield rather than upfield, as expected. For B2, all three $Co(CHEL)CH_3$ electrophiles shift the ^{13}C signal in the direction opposite to that expected from protonation.

Our findings demonstrate that expressions to account for changes in chemical shifts as a function of R in organocobalt complexes must incorporate CHEL anisotropy. A rigid system may be required to assess all contributions fully since the anisotropic contribution of the CHEL portion of Co(CHEL) is not uniform in the equatorial plane and since rotation of L around the Co-L bond will lead to a family of conformations. The population distribution of these conformers may depend on the bulk of R as well as the solvent, the electronic effect of R (i.e., the length of the Co-L bond), etc. Ironically, since the position of the 5,6-dimethylbenzimidazole moiety in cobalamins is relatively fixed, the CHEL ligand contribution may be easier to assess than in model compounds. However, the sparsity and low accuracy of cobalamin X-ray structures make overall interpretation of shifts more complex for cobalamins. Clearly, NMR spectroscopy has given us greater insight into the properties of both models and cobalamins but a deeper understanding is needed before the conformation of B_{12} in holoenzymes can be interpreted by NMR methods.

Acknowledgment. This research was supported by NIH Grant GM 29225 to L.G.M. and by a grant from the MPI (Rome) to L.R. The purchase of the NMR instruments was supported in part by NSF departmental grants to Emory University. We are grateful to these organizations.

Supplementary Material Available: Tables of analytical data, additional NMR data, complete bond lengths and bond angles, hydrogen atom positional parameters, and general displacement expressions for compounds I and II, figures of the absolute-value-mode 2N NOE spectra of $[Me_3BzmCo((DO)(DOH)Me_2pn)CH_3]PF_6$ and of $[1\text{-}MeImdCo((DO)(DOH)Me_2pn)CH_3]PF_6$, and an identifying figure for ^1H NMR chemical shifts (ppm) of $[1\text{-}MeImdCo((DO)(DOH)Me_2pn)]PF_6$ in $CDCl_3$ (16 pages); tables of observed and calculated structure factors for compounds I and II (14 pages). Ordering information is given on any current masthead page.

Contribution from the Department of Applied Chemistry, Faculty of Engineering, Osaka University, Yamadaoka, Suita, Osaka 565, Japan

Spectroscopic and Electrical Properties of $VO(dmit)_2$ and $V(dmit)_3$ Anion Complexes and X-ray Crystal Structure of $[NMP]_2[V(dmit)_3]$ (dmit = 2-Thioxo-1,3-dithiole-4,5-dithiolate, NMP = *N*-Methylphenazinium)

Gen-etsu Matsubayashi,* Kazuki Akiba, and Toshio Tanaka

Received May 3, 1988

$V^{IV}O(dmit)_2$ and $V^{IV}(dmit)_3$ anion complexes were prepared. Although they are essentially insulators, their oxidized complexes $[N\text{-methylphenazinium}]_2[V(dmit)_3]$, $[tetrathiafulvalenium]_2[V(dmit)_3]$, and $[NBu^n_4]_{0.17}[V(dmit)_3]$ as well as $[N\text{-methylpyridinium}]_2[VO(dmit)_2]\cdot I_{4.2}$ and $[NBu^n_4]_2[V(dmit)_3]\cdot I_{5.4}$ exhibit semiconductive behavior with electrical conductivities of 1×10^{-8}–1×10^{-2} S cm^{-1}. Electronic, ESR, and X-ray photoelectron spectra of these complexes are discussed on the basis of interactions between the anion moieties. A single-crystal X-ray structure analysis of $[N\text{-methylphenazinium}]_2[V(dmit)_3]$, $[C_{13}H_{11}N_2]_2[V(C_3S_5)_3]$, revealed a distorted-octahedral geometry of the $V(dmit)_3$ anion and a layer packing of the anions in the crystal phase. The orthorhombic crystal, space group *Pbca*, has cell dimensions $a = 18.5299$ (6) Å, $b = 30.726$ (2) Å, $c = 14.826$ (1) Å, $V = 8441$ (1) Å^3, and $Z = 8$. Block-diagonal least-squares refinement based on 5601 independent reflections with $|F_o| > 3\sigma(F)$ yielded an R factor of 0.056.

Introduction

In the design of electrically conducting organic compounds, two- or three-dimensional molecular interactions have been focused upon since organic superconductors such as tetramethyltetraselenasulvalene (TMTSF)[1] and bis(ethylenedithio)tetrathiafulvalene (BEDT-TTF) salts[2] were reported. Metal complexes with the 2-thioxo-1,3-dithiole-4,5-dithiolate ligand ($dmit^{2-}$, A) form two- or three-dimensional conduction pathways through contacts between the ligand sulfur atoms in the crystal phase. Several $(dmit)_2$metalate anion complexes (M = Ni, Pd, Pt) with high electrical conductivities have been reported,[3] of which $[TTF][Ni(dmit)_2]_2$ (TTF = tetrathiafulvalene) becomes a superconductor, although only under pressure and at low temperature.[3b,4]

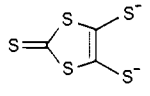

A

(1) For a review, see: Williams, J. M.; Carneiro, K. *Adv. Inorg. Chem. Radiochem.* **1985**, *29*, 249.

(2) (a) Urayama, H.; Yamochi, H.; Saito, G.; Nozawa, K.; Sugano, T.; Kinoshita, M.; Sato, S.; Oshima, K.; Kawamoto, A.; Tanaka, J. *Chem. Lett.* **1988**, 55 and references therein. (b) Urayama, H.; Yamochi, H.; Saito, G.; Sato, S.; Kawamoto, A.; Tanaka, J.; Mori, T.; Maruyama, Y.; Inokuchi, H. *Chem. Lett.* **1988**, 463.

(3) (a) Papavassiliou, G. C. *Z. Naturforsch., B* **1982**, *37*, 825. Valade, L.; Bousseau, M.; Gleizes, A.; Cassoux, P. *J. Chem. Soc., Chem. Commun.* **1983**, 110. Valade, L.; Cassoux, P.; Gleizes, A.; Interrante, L. *J. Phys., Colloq.* **1983**, *C3*, 1183. Valade, L.; Legos, J.-P.; Bousseau, M.; Cassoux, P.; Garbauskas, M.; Interrante, L. V. *J. Chem. Soc., Dalton Trans.* **1985**, 783. Bousseau, M.; Valade, L.; Bruniquel, M.-F.; Cassoux, P.; Garbauskas, M.; Interrante, L.; Kasper, J. *Nouv. J. Chim.* **1984**, *8*, 3. Kato, R.; Mori, T.; Kobayashi, A.; Sasaki, Y.; Kobayashi, H. *Chem. Lett.* **1984**, 1. Kato, R.; Kobayashi, H.; Kobayashi, A.; Sasaki, Y. *Chem. Lett.* **1984**, 191. Kim, H.; Kobayashi, A.; Sasaki, Y.; Kato, R.; Kobayashi, H. *Chem. Lett.* **1987**, 1799. (b) Bousseau, M.; Valade, L.; Legros, J.; Cassoux, P.; Garbauskas, M.; Interrante, L. V. *J. Am. Chem. Soc.* **1986**, *108*, 1908. Brossard, L.; Ribault, M.; Bousseau, M.; Valade, L.; Cassoux, P. *C. R. Acad. Sci., Ser. 2* **1986**, *302*, 205.

0020-1669/88/1327-4744$01.50/0

Cubic $(dmit)_3$ metalate anion complexes and other nonplanar $(dmit)_2$ oxometalate analogues also are expected to behave as new conductors upon oxidation through multidimensional dmit–dmit interactions in the solid.

This paper reports the preparation and spectroscopic and electrical properties of $V^{IV}O(dmit)_2$ and $V^{IV}(dmit)_3$ complexes and their oxidized analogues. The crystal structure of $[NMP]_2[V(dmit)_3]$ is also described.

Experimental Section

Materials. 4,5-Bis(benzoylthio)-1,3-dithiole-2-thione,[5] *N*-methylacridinium perchlorate ([NMA][ClO_4]),[6] *N*-methylpyridinium perchlorate ([Me-py][ClO_4]),[6] $[NBu^n_4]_2[Zn(dmit)_2]$,[5] and tris(tetrathiafulvalenium) bis(tetrafluoroborate) ($[TTF]_3[BF_4]_2$)[7] were prepared according to the literature. *N*-Methylphenazinium methyl sulfate ([NMP][$MeSO_4$]) and bis(acetylacetonato)oxovanadium ($VO(acac)_2$) were commercially available.

Preparation of $[Me\text{-}py]_2[VO(dmit)_2]$ (1). 4,5-Bis(benzoylthio)-1,3-dithiole-2-thione (400 mg, 1.0 mmol) was dissolved in a methanol (10 mL) solution together with sodium metal (65 mg, 2.8 mmol). A methanol (5 mL) solution of $VO(acac)_2$ (130 mg, 500 μmol) was stirred into the solution, followed by addition of a methanol (5 mL) solution of [Me-py][ClO_4] (220 mg, 1.2 mmol). Immediately, orange crystals of complex **1** precipitated, which were filtered, washed with water and methanol, and dried in vacuo (34% yield). Anal. Calcd for $C_{18}H_{16}N_2OS_{10}V$: C, 33.37; H, 2.49; N, 4.33. Found: C, 33.18; H, 2.43; N, 4.25.

Preparation of $[NBu^n_4]_2[V(dmit)_3]$ (3). To an acetonitrile (10 mL) solution of $[NBu^n_4]_2[Zn(dmit)_2]$ (390 mg, 420 μmol) was added VCl_3 (70 mg, 440 μmol), and the solution was stirred for 1 h at room temperature. After the undissolved material was filtered off, the filtrate was allowed to stand in a refrigerator overnight to afford red-brown needles of **3** (26% yield). Anal. Calcd for $C_{41}H_{72}N_2S_{15}V$: C, 43.77; H, 6.46; N, 2.49. Found: C, 42.99; H, 6.27; N, 2.56.

Preparation of $[NMA]_2[V(dmit)_3]$ (4). An acetonitrile (10 mL) solution of [NMA][ClO_4] (10 mg, 52 μmol) was added to an acetonitrile (10 mL) solution of **3** (21 mg, 18 μmol), and the solution was allowed to stand in a refrigerator overnight to give a dark green precipitate of **4** (30% yield). Anal. Calcd for $C_{37}H_{24}N_2S_{15}V$: C, 43.21; H, 2.36; N, 2.72. Found: C, 44.88; H, 2.33; N, 2.54.

Preparation of $[NMP]_2[V(dmit)_3]$ (5). An acetonitrile (10 mL) solution of **3** (21 mg, 18 μmol) was mixed with an acetonitrile (10 mL) solution of [NMP][$MeSO_4$] (12 mg, 39 μmol), and the solution was allowed to stand in a refrigerator for 2 days to yield dark green plates of **5** (43% yield). Anal. Calcd for $C_{35}H_{22}N_4S_{15}V$: C, 40.80; H, 2.16; N, 5.44. Found: C, 40.78; H, 2.26; N, 5.44.

Preparation of $[TTF]_2[V(dmit)_3]$ (6). An acetonitrile (5 mL) solution of **3** (11 mg, 10 μmol) was added with stirring to an acetonitrile (5 mL) solution of $[TTF]_3[BF_4]_2$ (14 mg, 17 μmol) to give a black precipitate. The mixture was further stirred for 1 h. The product (**6**) was separated by centrifugation, washed with diethyl ether, and dried in vacuo (57% yield based on **3**). Anal. Calcd for $C_{21}H_8S_{23}V$: C, 24.05; H, 0.77. Found: C, 23.51; H, 1.02.

Preparation of $[NBu^n_4]_{0.17}[V(dmit)_3]$ (7) by Electrocrystallization. An acetone (10 mL) solution containing both **3** (17 mg, 15 μmol) and $[NBu^n_4][ClO_4]$ (360 mg, 1.1 mmol) was subjected to a controlled-current (5-μA) electrolysis under a nitrogen atmosphere in a cell consisting of a platinum wire (anode) and a carbon rod (cathode). Black microcrystals of **7** thus produced on the anode were collected and dried in vacuo (31% yield). Anal. Calcd for $C_{11.7}H_{6.1}N_{0.17}V$: C, 20.63; H, 0.91; N, 0.35. Found: C, 21.02; H, 1.13; N, <0.3.

Iodine Doping of Complexes 1 and 3. Finely powdered complex **1** (50 mg, 77 μmol) was suspended in a hexane (20 mL) solution of iodine (58 mg, 230 μmol), and the suspension was stirred 1 h at room temperature under a nitrogen atmosphere. The resulting solid $[Me\text{-}py]_2[VO(dmit)_2]\cdot I_{4.2}$ (**2**) was washed with hexane, collected by filtration, and dried in vacuo (yield 90 mg). Anal. Calcd for $C_{18}H_{16}N_2OS_{10}I_{4.2}V$: C, 18.51; H, 1.38; N, 2.40. Found: C, 18.41; H, 1.55; N, 2.31.

By a similar procedure, $[NBu^n_4]_2[V(dmit)_3]\cdot I_{5.4}$ (**8**) was obtained by a reaction of **3** suspended in hexane with 3 molar equiv of iodine. Anal. Calcd for $C_{41}H_{72}N_2S_{15}I_{5.4}V$: C, 27.20; H, 4.02; N, 1.55. Found: C, 26.99; H, 4.22; N, 1.64.

Table I. Crystallographic Data for $[NMP]_2[V(dmit)_3]$ (**5**)

chem formula: $C_{35}H_{22}N_4S_{15}V$	T = 23 °C
fw = 1030.43	λ = 1.5418 Å
space group: *Pbca* (No. 61)	d_{calcd} = 1.620 (1) g cm^{-3}
a = 18.5299 (6) Å	μ = 89.7 cm^{-1}
b = 30.726 (2) Å	transmission coeff: 1.00–0.33
c = 14.826 (1) Å	$R(F_o)$ = 0.056
V = 8441 (1) Å^3	$R_w(F_o^2)$ = 0.071
Z = 8	

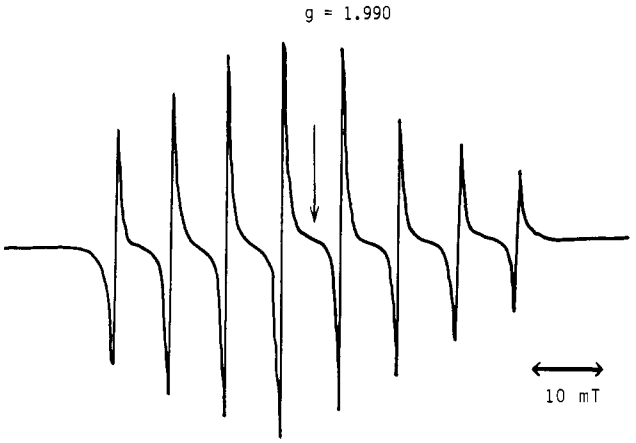

Figure 1. ESR spectrum of **1** in acetonitrile at room temperature.

Measurements. Specific resistivities were measured for compacted pellets in the −35 to +35 °C range by the conventional two-probe method.[8] Electronic absorption, powder reflectance,[8] ESR and X-ray photoelectron (XPS),[9] and Raman spectra[10] were recorded as described previously. Electronic absorption spectra under a controlled-potential electrolysis were recorded by using an electrolysis cell having a platinum-mesh electrode that was modified according to the literature.[11] Cyclic voltammograms of the complexes were recorded in acetone and in acetonitrile as described previously.[10]

X-ray Crystal Structure Determination of $[NMP]_2[V(dmit)_3]$ (5). Oscillation and Weissenberg photographs indicated an orthorhombic system, and the space group *Pbca* was confirmed from the successful analysis. Accurate unit-cell parameters were determined from 25 reflections with 2θ values from 44 to 46°, measured with a Rigaku four-circle diffractometer at the Crystallographic Research Center, Institute for Protein Research, Osaka University.

Crystallographic data for **5** are summarized in Table I (see supplementary material for data collection parameters).

Throughout the data collection no significant intensity variation was observed. The intensities were corrected for Lorentz and polarization effects as well as absorption.[12] A total of 6731 unique reflections was measured, of which 5601 with $|F_o| > 3\sigma(F)$ were used for the structure determination. Coordinates of vanadium and sulfur atoms were found according to the direct (MULTAN) method.[13] By successive Fourier calculations, positions of all the non-hydrogen atoms were found. Although hydrogen atoms of the methyl groups of the NMP moieties were not determined, positions of ring hydrogen atoms of the NMP moieties were clarified from a difference Fourier map based on the anisotropic refinement of all the non-hydrogen atoms. Block-diagonal least-squares refinement was carried out with anisotropic thermal parameters for all the non-hydrogen atoms and with isotropic thermal parameters for the clarified hydrogen atoms. Atomic scattering factors used throughout the refinement were taken from ref 14. The final atomic positional and

(4) Recently $[NMe_4][Ni(dmit)_2]_2$ was reported to become a superconductor with a quasi-one-dimensionality: Kobayashi, A.; Kim, H.; Sasaki, Y.; Kato, R.; Kobayashi, H.; Moriyama, S.; Nishio, Y.; Kajita, K.; Sasaki, W. *Chem. Lett.* **1987**, 1819.
(5) Steimecke, G.; Sieler, H.-J.; Kirmse, R.; Hoyer, E. *Phosphorus Sulfur* **1979**, *7*, 49.
(6) Tanaka, H.; Matsubayashi, G.; Tanaka, T. *Bull. Chem. Soc. Jpn.* **1984**, *57*, 2198.
(7) Wudl, F. *J. Am. Chem. Soc.* **1975**, *79*, 1962.
(8) Ueyama, K.; Matsubayashi, G.; Tanaka, T. *Inorg. Chim. Acta* **1984**, *87*, 143.
(9) Matsubayashi, G.; Kondo, K.; Tanaka, T. *Inorg. Chim. Acta* **1983**, *69*, 167.
(10) Matsubayashi, G.; Takahashi, K.; Tanaka, T. *J. Chem. Soc., Dalton Trans.* **1988**, 967.
(11) Lexa, D.; Savent, J. M.; Zicker, J. *J. Am. Chem. Soc.* **1977**, *99*, 2786.
(12) North, A. C. T.; Phillips, D. C.; Matheus, F. C. *Acta Crystallogr.* **1968**, *A24*, 351.
(13) Main, M.; Hull, S. E.; Lessinger, L.; Germain, G.; Declercq, J.-P.; Woolfson, M. M. "A System of Computer Programs for the Automatic Solution of Crystal Structures from X-Ray Diffraction Data, MULTAN 78"; University of York: York, England, 1978.
(14) *International Tables for X-Ray Crystallography*; Kynoch: Birmingham, England, 1974; Vol. 4.

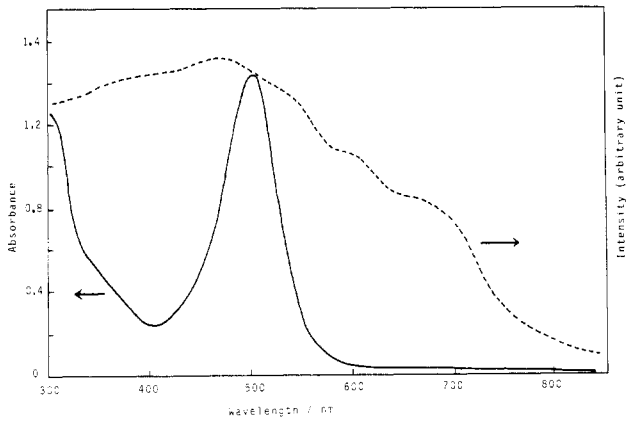

Figure 2. Electronic absorption spectrum of **1** (1.0×10^{-4} mol L^{-1}) in acetonitrile and its powder reflectance spectrum at room temperature.

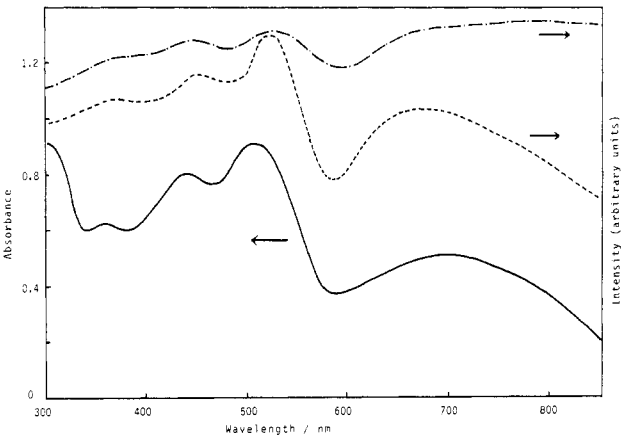

Figure 3. Electronic absorption spectrum of **3** (1.0×10^{-4} mol L^{-1}) in acetonitrile (—) and powder reflectance spectra of **3** (- - -) and **4** (-·-) at room temperature.

thermal parameters with standard deviations are given in Table II. Crystallographic calculations were performed by using the programs developed by Prof. K. Nakatsu, Kwansei Gakuin University, on an ACOS 900S computer at the Crystallographic Research Center, Institute for Protein Research, Osaka University. Figures 7 and 8 were drawn with a local version of ORTEP-II.[15]

Results and Discussion

Spectroscopic and Electrochemical Properties of Complexes 1, 3, and 4. Figure 1 shows the ESR spectrum of complex **1** measured in acetonitrile at room temperature. The spectrum consists of eight hyperfine structure lines due to the interaction of the unpaired electron with the ^{51}V nuclear spin ($I = {}^7/_2$, 100%). Complexes **3** and **4** also have shown similar solution spectra.

The isotropic g values and hyperfine coupling parameters a_0(^{51}V) are $g = 1.990$ and $a_0 = 77.5 \times 10^{-4}$ cm^{-1} for **1**, $g = 1.980$ and $a_0(^{51}V) = 63.4 \times 10^{-4}$ cm^{-1} for **3** (lit.:[16] $g = 1.979$, $a_0 = 63.9 \times 10^{-4}$ cm^{-1} in acetone), and $g = 1.980$ and $a_0(^{51}V) = 65.7 \times 10^{-4}$ cm^{-1} for **4**. These data indicate the vanadium(IV) valence state of these complexes. The hyperfine V coupling constant of **1** is close to that of $[NMe_4]Na[VO(SCH_2CH_2S)_2]$ ($a_0 = 75 \times 10^{-4}$ cm^{-1})[17] and is smaller than that ($a_0 = 82 \times 10^{-4}$ cm^{-1}) of the $[VO(cat)_2]^{2-}$ complex (cat = catecholate) in water,[18] and the coupling constants of **3** and **4** are also smaller than that (75×10^{-4} cm^{-1}) of the $[V(cat)_3]^{2-}$ complex in acetonitrile.[18] These findings may suggest an extended delocalization of vanadium 3d electrons to the dmit ligands, which is consistent with the occurrence of a ligand-centered oxidation of the $V(dmit)_3$ anion as described later.

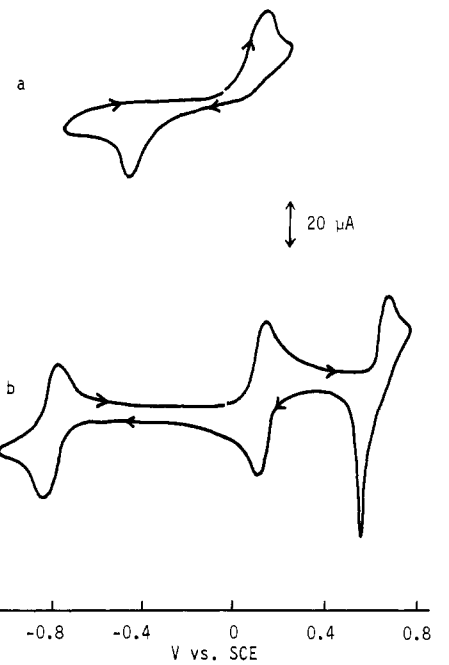

Figure 4. Cyclic voltammograms of (a) **1** (1.0×10^{-3} mol L^{-1}) in acetone and (b) **3** (5.0×10^{-4} mol L^{-1}) in acetonitrile at room temperature (0.1 mol L^{-1} $[NBu^n_4][ClO_4]$, sweep rate 0.1 V s^{-1}).

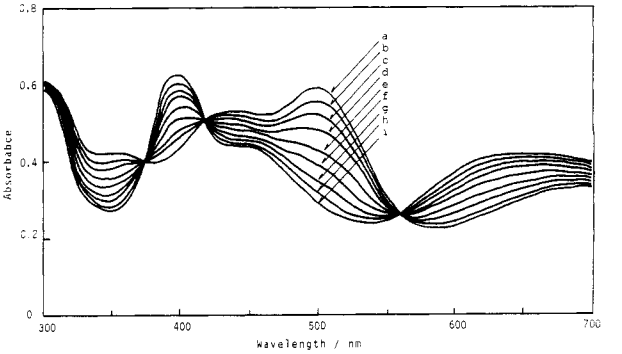

Figure 5. Electronic absorption spectra of **3** during controlled-potential electrolysis (0.3 V vs SCE) in acetonitrile (0.1 mol L^{-1} $[NBu^n_4][ClO_4]$) Electrolysis time (min): (a) 0; (b) 3; (c) 9; (d) 15; (e) 21; (f) 27; (g) 33; (h) 39; (i) 45.

The electronic absorption spectrum in acetonitrile and the powder reflectance spectrum of **1** are illustrated in Figure 2. The intense absorption band at 505 nm is due to the dmit π–π^* transition as was observed for Na_2dmit (514 nm in methanol), $[NBu^n_4]_2[Zn(dmit)_2]$ (530 nm in acetonitrile), and [*N*-ethylpyridinium]$_2$[Cu(dmit)$_2$] (540 nm in acetonitrile).[10] On the other hand, the reflectance spectrum shows other broad bands near 700 nm, suggesting some interanionic interaction in the solid state. Figure 3 shows the absorption spectrum of **3** in acetonitrile together with the powder reflectance spectra of **3** and **4**. The intense band at 505 nm observed in the absorption spectrum of **3** seems to be also associated with the dmit π–π^* transition. The solid-state spectrum of **3** is essentially the same as that in solution, indicating no interaction among the anions separated by the tetrabutylammonium cation moieties, as was observed for the crystal structure of $[NBu^n_4]_2[V(dmt)_3]$.[16] On the other hand, the solid-state spectrum of **4** indicates a broad reflectance band around 800 nm, which may be due to an interaction among the anion moieties.

Cyclic voltammograms of **1** in acetonitrile and of **3** in acetone are illustrated in Figure 4. Although complex **1** can be oxidized at a low potential (anode peak potential 0.19 V vs SCE), the

(15) Johnson, C. K. "ORTEP-II"; Report ORNL 5138; Oak Ridge National Laboratory: Oak Ridge, TN, 1976.
(16) Oak, R.-M.; Dietzsch, W.; Kirmse, R.; Stach, J.; Hoyer, E. *Inorg. Chim. Acta* **1984**, *128*, 251.
(17) Wiggins, R. W.; Huffman, J. C.; Christou, G. *J. Chem. Soc., Chem. Commun.* **1983**, 1313.
(18) Cooper, S. R.; Koh, Y. B.; Raymond, K. N. *Inorg. Chem.* **1982**, *104*, 5092.

Table II. Atomic Positional and Thermal Parameters for $[NMP]_2[V(dmit)_3]$ (**5**)

atom	x	y	z	U_{iso}, Å^2	atom	x	y	z	U_{iso}, Å^2
V	0.49470 (4)	0.15395 (2)	0.20239 (5)	0.0303 (3)	C(17)	0.8851 (4)	0.4198 (2)	0.0997 (4)	0.090 (5)
S(1)	0.41688 (6)	0.13628 (4)	0.32539 (8)	0.0355 (7)	C(18)	0.9515 (4)	0.4340 (2)	0.0777 (5)	0.104 (6)
S(2)	0.57934 (6)	0.17184 (4)	0.31737 (8)	0.0343 (5)	C(19)	1.0078 (4)	0.4049 (3)	0.0659 (4)	0.079 (5)
S(3)	0.57688 (8)	0.17178 (5)	0.52152 (9)	0.0682 (9)	C(20)	0.9983 (3)	0.3612 (2)	0.0767 (4)	0.053 (4)
S(4)	0.5137 (1)	0.15147 (5)	0.7009 (1)	0.1252 (16)	C(21)	0.9297 (3)	0.3448 (2)	0.0988 (3)	0.058 (3)
S(5)	0.43382 (8)	0.13544 (5)	0.52936 (9)	0.0635 (9)	C(22)	0.9727 (4)	0.2687 (2)	0.0883 (4)	0.073 (4)
S(6)	0.38674 (6)	0.14039 (4)	0.12136 (8)	0.0365 (7)	C(23)	0.7520 (3)	0.0080 (2)	0.3402 (4)	0.044 (3)
S(7)	0.47097 (7)	0.22869 (4)	0.17247 (9)	0.0358 (7)	C(24)	0.8259 (3)	0.0209 (2)	0.3398 (5)	0.054 (4)
S(8)	0.33402 (7)	0.27619 (4)	0.1224 (1)	0.0468 (7)	C(25)	0.8767 (3)	−0.0095 (2)	0.3176 (5)	0.052 (4)
S(9)	0.18062 (9)	0.28144 (6)	0.0643 (1)	0.0549 (9)	C(26)	0.8584 (4)	−0.0521 (2)	0.2914 (5)	0.059 (4)
S(10)	0.25645 (7)	0.19709 (5)	0.08517 (9)	0.0348 (7)	C(27)	0.7880 (3)	−0.0649 (2)	0.2894 (4)	0.055 (4)
S(11)	0.51943 (7)	0.07888 (4)	0.17378 (9)	0.0411 (7)	C(28)	0.7329 (3)	−0.0353 (2)	0.3148 (4)	0.051 (3)
S(12)	0.59823 (6)	0.16792 (4)	0.11407 (8)	0.0369 (5)	C(29)	0.6135 (3)	−0.0219 (2)	0.3397 (4)	0.045 (3)
S(13)	0.72927 (7)	0.11217 (5)	0.0709 (1)	0.0371 (7)	C(30)	0.5405 (3)	−0.0369 (2)	0.3415 (4)	0.054 (3)
S(14)	0.80861 (9)	0.02777 (6)	0.0576 (1)	0.0576 (9)	C(31)	0.4876 (3)	−0.0103 (2)	0.3712 (4)	0.050 (3)
S(15)	0.65732 (8)	0.03334 (4)	0.1223 (1)	0.0558 (9)	C(32)	0.5033 (3)	0.0321 (2)	0.3989 (4)	0.052 (3)
N(1)	0.9148 (2)	0.3011 (1)	0.1071 (3)	0.061 (3)	C(33)	0.5709 (3)	0.0486 (2)	0.3974 (4)	0.056 (4)
N(2)	0.8059 (3)	0.3622 (1)	0.1367 (3)	0.063 (3)	C(34)	0.6284 (3)	0.0217 (2)	0.3676 (4)	0.050 (3)
N(3)	0.6980 (3)	0.0357 (1)	0.3636 (3)	0.052 (3)	C(35)	0.7147 (4)	0.0824 (2)	0.3873 (7)	0.067 (4)
N(4)	0.6646 (2)	−0.0494 (1)	0.3136 (3)	0.051 (3)	H(11)	0.865 (4)	0.220 (2)	0.128 (5)	0.08 (3)
C(1)	0.4682 (3)	0.1460 (2)	0.4210 (3)	0.050 (3)	H(12)	0.740 (4)	0.201 (3)	0.193 (5)	0.07 (2)
C(2)	0.5351 (3)	0.1620 (2)	0.4181 (3)	0.049 (3)	H(13)	0.664 (4)	0.257 (2)	0.202 (4)	0.07 (2)
C(3)	0.5087 (3)	0.1527 (2)	0.5889 (4)	0.081 (4)	H(14)	0.689 (4)	0.338 (2)	0.187 (4)	0.05 (2)
C(4)	0.3464 (3)	0.1908 (2)	0.1184 (3)	0.034 (2)	H(17)	0.847 (3)	0.441 (2)	0.108 (4)	0.05 (2)
C(5)	0.3827 (3)	0.2280 (2)	0.1364 (3)	0.044 (3)	H(18)	0.956 (4)	0.469 (3)	0.063 (5)	0.09 (3)
C(6)	0.2527 (3)	0.2531 (2)	0.0890 (3)	0.049 (3)	H(19)	1.050 (4)	0.415 (2)	0.057 (4)	0.05 (2)
C(7)	0.6072 (3)	0.0808 (2)	0.1345 (3)	0.043 (3)	H(20)	1.032 (3)	0.347 (2)	0.069 (3)	0.02 (2)
C(8)	0.6407 (3)	0.1178 (2)	0.1105 (3)	0.037 (3)	H(24)	0.838 (4)	0.054 (2)	0.363 (5)	0.06 (2)
C(9)	0.7351 (3)	0.0567 (2)	0.0816 (4)	0.055 (4)	H(25)	0.926 (3)	0.003 (2)	0.317 (4)	0.04 (2)
C(10)	0.8474 (3)	0.2878 (2)	0.1310 (3)	0.064 (4)	H(26)	0.897 (3)	−0.075 (2)	0.285 (3)	0.03 (2)
C(11)	0.8294 (4)	0.2432 (2)	0.1412 (4)	0.083 (4)	H(27)	0.767 (3)	−0.094 (2)	0.292 (4)	0.05 (2)
C(12)	0.7616 (4)	0.2318 (2)	0.1660 (4)	0.102 (5)	H(30)	0.538 (5)	−0.065 (3)	0.306 (5)	0.09 (3)
C(13)	0.7066 (4)	0.2637 (2)	0.1826 (4)	0.071 (4)	H(31)	0.437 (3)	−0.020 (2)	0.366 (4)	0.06 (2)
C(14)	0.7227 (3)	0.3064 (2)	0.1737 (4)	0.056 (4)	H(32)	0.468 (3)	0.047 (2)	0.414 (4)	0.05 (2)
C(15)	0.7930 (3)	0.3198 (2)	0.1470 (3)	0.060 (3)	H(33)	0.581 (3)	0.078 (2)	0.410 (4)	0.06 (2)
C(16)	0.8724 (3)	0.3747 (2)	0.1120 (4)	0.060 (3)					

process is irreversible. On the other hand, complex **3** shows reversible oxidation waves ($E_{1/2}° = 0.15$ and 0.65 V vs SCE) that correspond to the redox processes $[V(dmit)_3]^{2-}/[V(dmit)_3]^-$ and $[V(dmit)_3]^-/[V(dmit)_3]^0$, respectively. Moreover, it displays a reversible redox wave due to $[V(dmit)_3]^{3-}/[V(dmit)_3]^{2-}$ at −0.78 V vs SCE.

The stable oxidation process of the $[V(dmit)_3]^{2-}$ anion is also shown in a reversible change of absorption bands in its visible spectrum under the electrolysis (Figure 5). The intense band at 500 nm decays on the controlled-potential oxidation at 0.30 V vs SCE, a band concomitantly occurring at 390 nm. On the subsequent reduction at −0.10 V vs SCE the original spectrum is recovered. In the second redox process, a reversible spectral change has also been observed; when the controlled-potential oxidation is performed at +0.80 V vs SCE, all the bands appreciably lessen in their intensities, probably due to adsorption of a further oxidized species upon a platinum-mesh electrode, and when the reduction is performed at +0.40 V vs SCE, the bands due to the $[V(dmit)_3]^-$ ion are recovered.

Oxidized dmit–Vanadium Complexes. The dmit–vanadium(IV) complexes have been oxidized by iodine. **1** and **3** have been doped with iodine by reactions of the finely powdered complexes suspended in hexane with an excess amount of iodine. The complexes obtained, **2** and **8**, give a Raman peak at 108 and 106 cm^{-1}, respectively, which is assignable to the symmetric stretching of the I_3^- ion.[19] The oxidation state of the dmit–vanadium complexes can be deduced from the dmit C=C stretching frequency. The infrared bands of **1** and **3** appear at 1440 and 1430 cm^{-1}, respectively, whereas both **2** and **8** give a strong band at 1330 cm^{-1} as well as very weak bands at the original frequencies of **1** and **3**. The appearance of the band lowered by ca. 100 cm^{-1} suggests the presence of one-electron-oxidized dmit–vanadium moieties.[20] Thus, **2** and **8** seem to contain essentially one-electron-oxidized dmit–vanadium moieties.

Although the $[VO(dmit)_2]^{2-}$ anion is irreversibly oxidized, the $[V(dmit)_3]^{2-}$ anion can be easily and stably oxidized by chemical and electrochemical processes to yield the stable complexes **5**–**7**.

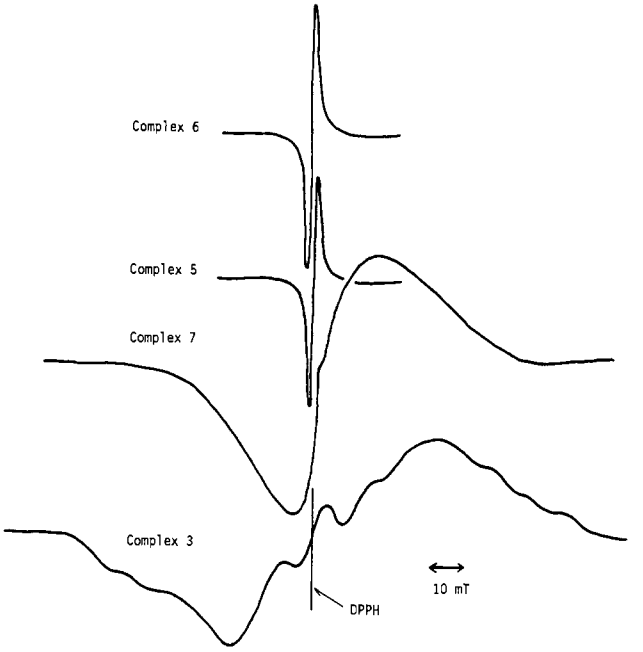

Figure 6. Powder ESR spectra of **3**, **5**, **6**, and **7** at room temperature.

(19) Cowie, M. A.; Cleizes, A.; Grynnkewich, G. W.; Kalina, D. W.; McClure, M. S.; Scaaringe, R. D.; Teitelbaum, R. C.; Ruby, S. L.; Ibers, J. A.; Kannewurf, C. R.; Marks, T. J. *J. Am. Chem. Soc.* **1979**, *101*, 2921.

(20) Sakamoto, Y.; Matsubayashi, G.; Tanaka, T. *Inorg. Chim. Acta* **1986**, *113*, 137.

Table III. Binding Energies of V $2p_{1/2}$ Electrons (eV)

complex		complex	
1	523.4	**5**	523.4
2	524.7	**6**	522.3
3	523.3	**7**	524.7
4	523.2	**8**	524.3

Table IV. Bond Distances (Å) and Angles (deg) Relevant to the Vanadium Coordination Sphere of $[NMP]_2[V(dmit)_3]$ (**5**)

V-S(1)	2.387 (1)	V-S(2)	2.381 (1)
V-S(6)	2.370 (1)	V-S(7)	2.380 (1)
V-S(11)	2.390 (1)	V-S(12)	2.362 (1)
S(1)-V-S(2)	84.46 (5)	S(1)-V-S(6)	84.64 (5)
S(1)-V-S(7)	104.5 (1)	S(1)-V-S(11)	91.83 (5)
S(1)-V-S(12)	162.8 (1)	S(2)-V-S(6)	163.6 (1)
S(2)-V-S(7)	91.86 (5)	S(2)-V-S(11)	102.9 (1)
S(2)-V-S(12)	79.63 (5)	S(6)-V-S(7)	85.37 (5)
S(6)-V-S(11)	84.39 (5)	S(6)-V-S(12)	115.9 (1)
S(7)-V-S(11)	159.0 (1)	S(7)-V-S(12)	82.61 (5)
S(11)-V-S(12)	85.48 (5)	V-S(1)-C(1)	104.7 (2)
V-S(2)-C(2)	105.4 (2)	V-S(6)-C(4)	102.8 (2)
V-S(7)-C(5)	102.8 (2)	V-S(11)-C(7)	102.0 (2)
V-S(12)-C(8)	103.0 (2)		

5 and **6** show the dmit ν(C=C) stretching band at 1340 and 1330 cm^{-1}, respectively, indicating the presence of the $[V(dmit)_3]^-$ anion. On the other hand, complex **7** obtained by the electrochemical oxidation exhibits two ν(C=C) bands at 1330 and 1250 cm^{-1}, which suggests the presence of both $[V(dmit)_3]^-$ and $[V(dmit)_3]^0$ in the solid state.

Figure 6 shows the powder ESR spectra of **5**–**7** as well as that of **3**. Although the signal of **3** is very broad due to the presence of one d electron in the V(IV) state, the signals of **5** and **6** are sharp with g values of 2.002 and 2.008, respectively. Since the $[V(dmit)_3]^-$ anion is ESR-silent, these signals surely come from the $NMP^{\bullet}$ radical for **5** and the $TTF^{\bullet+}$ radical cation for **6**. Complex **7** containing the $[V(dmit)_3]^0$ moieties shows a broad, approximately isotropic signal (g = 1.966).

Complex **6** exhibits a Raman peak at 1425 cm^{-1}, which is ascribed to a C=C stretching of the TTF moiety. The symmetric C=C stretching peak of TTF^0 occurs at 1500 cm^{-1},[21-23] while the corresponding peak of the $TTF^{\bullet+}$ radical cation appears at 1416 cm^{-1}.[22] Thus, the TTF moieties of complex **6** seem to be in a $TTF^{\bullet+}/TTF^0$ mixed state.

The valence state of the vanadium atom of the complexes can be deduced from binding energies of 2p electrons determined from XPS, which are summarized in Table III. Iodine-doped complexes **2** and **8** exhibit larger binding energies of the 2p electrons than those of **1** and **3**, respectively, suggesting noticeable oxidation of the metal. However, the binding energies of **5** and **7** are very close to those of **3** and **4**, indicating that essentially dmit ligand centered oxidation occurs. On the other hand, complex **6** shows an appreciably small binding energy compared with that of **3**. Such a lowered binding energy seems to suggest a charge transfer from $TTF^{\bullet+}/TTF^0$ moieties to the $V(dmit)_3$ moieties through sulfur–sulfur interactions. This is similar to charge-transfer interactions from TTF sulfur to $[SnCl_6]^{2-}$ and to $[PtCl_6]^{2-}$ anions reported for $[TTF]_3[SnCl_6]$[24] and $[TTF]_3[PtCl_6]$,[25] where binding energies of Sn 3d and Pt 4f electrons of these complexes are also smaller than those of $[NBu^n_4]_2[SnCl_6]$ and $[NBu^n_4]_2[PtCl_6]$, respectively.

Crystal Structure of $[NMP]_2[V(dmit)_3]$ (5). The crystal structure of **5** consists of 16 NMP moieties and 8 $V(dmit)_3$ anions in the unit cell. Figure 7 shows the molecular geometries together with the atom-labeling scheme. Bond distances and angles relevant to the vanadium coordination sphere of the complex are listed in Table IV. Table V (see supplementary material) shows bond distances and angles for the dmit ligands and the NMP moieties. Six sulfur atoms are located around the vanadium atom at the average distance of 2.378 (4) Å. This is very close to the values reported for the tris(dithiolato)vanadium complexes such as $[NMe_4]_2[V(mnt)_3]$ (mnt = maleonitriledithiolate; 2.36 (1) Å)[26] and $[NBu^n_4]_2[V(dmt)_3]$ (dmt = 3-thioxo-1,2-dithiole-4,5-dithiolate; 2.375 (15) Å).[16]

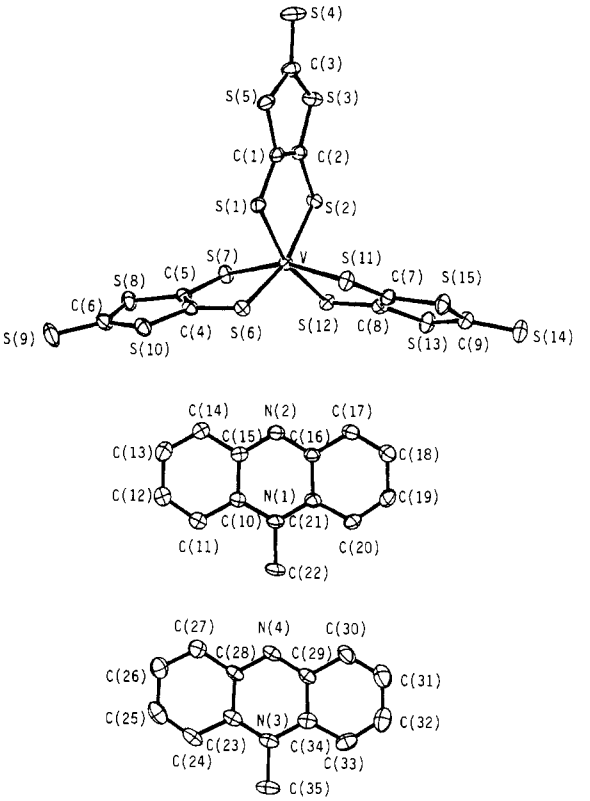

Figure 7. Geometries of the cations and the anion of **5** together with the atom-labeling scheme.

The S–V–S angles (S(1)–V–S(12), S(2)–V–S(6), and S(7)–V–S(11)) are averaged to 161.8 (11)°, which is appreciably lower than 175.1°, calculated for a corrected octahedron formed by rigid chelate ligands having an averaged S–V–S bite angle of 85.1 (3)°.[27] The value deviates remarkably from that of a trigonal prism, which is expected to be approximately 136°. Thus, the VS_6 core is considered to have a distorted-octahedral symmetry. This geometry is close to that of the VS_6 cores of $[NMe_4]_2[V(mnt)_3]$ (the pseudo trans angle S–V–S; 158.6°)[26] and of $[NBu^n_4]_2[V(dmt)_3]$ (S–V–S; 164.3 (12)°).[16] Owing to this distortion of the VS_6 core, the interligand S–S distances vary from 3.037 (2) to 3.769 (2) Å, although the averaged intraligand S–S distance is 3.217 (8) Å.

Vanadium and S(1)–S(5) atoms form a least-squares plane with the maximum deviation of ±0.05 Å of these atoms, while the vanadium atom deviates by 0.47 (5) and 0.51 (5) Å, respectively, from the least-squares planes consisting of S(6)–S(10) and S(11)–S(15) atoms of dmit ligands with the maximum deviations of ±0.05 and ±0.02 Å, respectively, of sulfur atoms. This remarkable vanadium deviation from the planar dithiolene ligands is rather close to that of $[N$-ethylpyridinium$]_2[Cu(dmit)_2]$ (the deviation of Cu from the dmit ligand plane is 0.27 (5) Å)[10] and is in contrast to the planarity of the vanadium atom and ligands observed for $[NMe_4]_2[V(mnt)_3]$[26] and $[NBu^n_4]_2[V(dmt)_3]$.[16]

The NMP moieties are planar (maximum deviations of atoms from the least-squares planes of 0.07 and 0.09 Å), and C–C and

(21) Bozio, R.; Girlando, A.; Pecile, D. *Chem. Phys. Lett.* **1977**, *52*, 503.
(22) Bozio, R.; Zanon, I.; Girlando, A.; Pecile, C. *J. Chem. Phys.* **1979**, *71*, 2282.
(23) Matsuzaki, S.; Moriyama, T.; Toyoda, K. *Solid State Commun.* **1980**, *34*, 857.
(24) Matsubayashi, G.; Ueyama, K.; Tanaka, T. *J. Chem. Soc., Dalton Trans.* **1985**, 465.
(25) Ueyama, K.; Matsubayashi, G.; Tanaka, T. *Inorg. Chim. Acta* **1986**, *112*, 135.
(26) Stiefel, E. I.; Dori, Z.; Gray, H. B. *J. Am. Chem. Soc.* **1967**, *89*, 3353.
(27) Cowie, M.; Bennett, M. J. *Inorg. Chem.* **1976**, *15*, 1595.

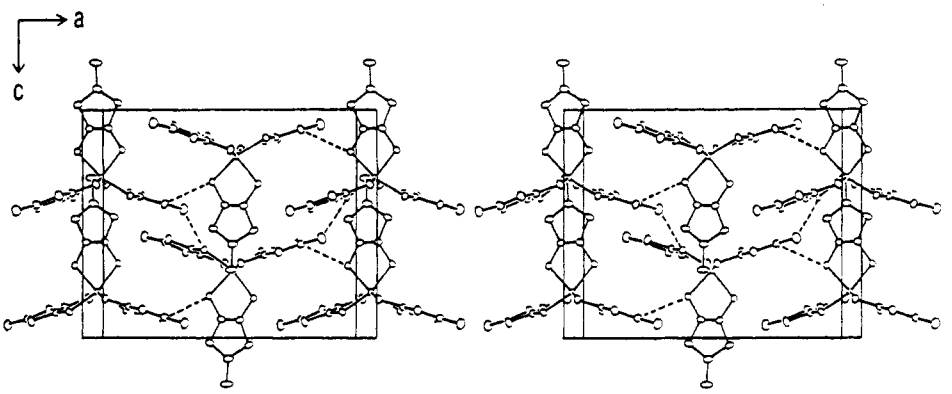

Figure 8. Stereoview of the packing diagram of the $V(dmit)_3$ anions of **5**. The dashed lines represent S–S nonbonded contacts less than 3.7 Å.

Table VI. Electrical Conductivities (σ) and Activation Energies (E_a)

complex	$\sigma_{25\,°C}$/S cm^{-1}	E_a/eV	complex	$\sigma_{25\,°C}$/S cm^{-1}	E_a/eV
1	3.8×10^{-10}	0.81	**5**	2.8×10^{-5}	0.24
2	5.2×10^{-7}	1.04	**6**	1.0×10^{-2}	0.15
3	4.5×10^{-10}	0.62	**7**	1.0×10^{-4}	0.38
4	3.4×10^{-8}	0.61	**8**	1.2×10^{-8}	0.95

C–N distances are close to those for the reported NMP complexes [NMP][TCNQ],[28] $[NMP]_2[TCNQ]_3$ (TCNQ = 7,7,8,8-tetracyano-*p*-quinodimethane),[29] and $[NMP]_2[Cu(mnt)_2]$.[30] In the present complex the NMP cations are partially reduced, exhibiting an ESR spectrum due to the NMP• radical, as described above. Although two crystallographically independent NMP moieties are present, no appreciable differences are observed in the interatomic distances for these two NMP molecules. They are located separately among the $V(dmit)_3$ anions without any significant contact between them. Some dmit sulfur atoms access the NMP carbons within the sum of van der Waals radii of their atoms (3.55 Å).[31] However, no dmit–dmit interaction between the anions is observed bridged with the NMP cations.

Figure 8 shows the packing diagram of the $V(dmit)_3$ anions, where the NMP moieties are not illustrated for simplicity. Some intermolecular S–S contacts within the sum of van der Waals radii (3.7 Å)[31] are observed in the crystal phase: S(9)---S(12)′ (3.427 (2) Å), S(10)---S(2)″ (3.669 (2) Å), and S(8)′---S(5)″ (3.563 (2) Å). Thus, a two-dimensional interaction among the anion moieties is deduced approximately along the *ac* plane. Such S–S interactions were reported for dmit–metal complexes such as partially oxidized $[M(dmit)_2]^{\delta-}$ (M = Ni, Pd, Pt; $\delta < 1$) complexes[3] and $[N$-ethylpyridinium$]_2[Cu(dmit)_2]$.[10] The interaction among the anions in the present complex seems to result in its semiconductive behavior, as described below.

Electrical Conductivities. The temperature dependence of the electrical resistivities of compacted samples has indicated that all the complexes behave as typical semiconductors in the −30 to +30 °C range. Table VI summarizes the electrical conductivities at 25 °C and activation energies for the electrical conduction. Although complexes **1** and **3** exhibit very small conductivities, the iodine-doped complexes **2** and **8** have somewhat raised conductivities. This may be due to extended molecular interactions among the oxidized dmit–vanadium anions.

Complex **4** also has a slightly raised conductivity presumably due to a suitable interaction among the anion moieties. Complexes **5**–**7** exhibit appreciably high conductivities. It is deduced from the crystal structure of **5** that the electrical conduction occurs in these complexes through molecular interaction between oxidized $V(dmit)_3$ anions. Particularly, **6** behaves as a good electrical conductor, which may come from the two- or three-dimensional molecular interaction among TTF and $V(dmit)_3$ moieties through sulfur–sulfur contacts.

Acknowledgment. We thank Professor K. Nakatsu, Kwansei Gakuin University, for use of the programs for the structure solution and refinement. This work was partially supported by a grant from the Material Science Research Foundation.

Supplementary Material Available: Table SI (crystallographic data and summary of data collection and refinement), Table V (all bond distances and angles), and a table listing anisotropic thermal parameters (18 pages); a table of calculated and observed structure factors (24 pages). Ordering information is given on any current masthead page.

(28) Fritchie, C. J., Jr. *Acta Crystallogr.* **1966**, *20*, 892.
(29) Sanz, F.; Daly, J. J. *J. Chem. Soc., Perkin Trans. 2* **1975**, 1146.
(30) Kuppusamy, P.; Ramakrishna, B. L.; Manoharan, P. T. *Inorg. Chem.* **1984**, *23*, 3886.
(31) Pauling, L. *The Nature of the Chemical Bond*, 3rd ed.; Cornell University Press: Ithaca, NY, 1960; p 246.